

## The Crystal Structures of Trimesic Acid, its Hydrates and Complexes. II.\* Trimesic Acid Monohydrate— $\frac{2}{3}$ Picric Acid and Trimesic Acid $\frac{5}{6}$ Hydrate

BY F. H. HERBSTEIN†

*Department of Chemistry, Technion—Israel Institute of Technology, Haifa, Israel*

AND R. E. MARSH

*Arthur Amos Noyes Laboratory of Chemical Physics,‡ California Institute of Technology, Pasadena, California 91125, USA*

(Received 12 October 1976; accepted 22 January 1977)

The crystal structures of trimesic acid monohydrate— $\frac{2}{3}$  picric acid [TMA·H<sub>2</sub>O· $\frac{2}{3}$ PA, triclinic,  $a = 18.269$  (8),  $b = 8.852$  (5),  $c = 3.642$  (4) Å,  $\alpha = 90.43$  (8),  $\beta = 92.59$  (6),  $\gamma = 99.56$  (5)°,  $P\bar{1}$ ,  $Z = 2$ ] and trimesic acid  $\frac{5}{6}$  hydrate [TMA· $\frac{5}{6}$ H<sub>2</sub>O, triclinic,  $a = 16.640$  (1),  $b = 18.548$  (1),  $c = 9.512$  (1) Å,  $\alpha = 95.81$  (1),  $\beta = 91.06$  (4),  $\gamma = 94.35$  (1)°,  $P1$ ,  $Z = 12$ ] were determined by standard four-circle diffractometer techniques (Mo  $K\alpha$ ; 2840 and 6768 non-zero reflections respectively). In TMA·H<sub>2</sub>O· $\frac{2}{3}$ PA there are hydrogen-bonded layers of composition TMA·H<sub>2</sub>O in the (111) planes; these layers are pierced by channels along [001] containing the picric acid molecules. Diffuse X-ray scattering by these crystals suggests that the enclathrated picric acid molecules have only a short-range coherence with the TMA·H<sub>2</sub>O layers. TMA· $\frac{5}{6}$ H<sub>2</sub>O contains very similar layers of TMA·H<sub>2</sub>O in the (100) planes; the five such layers in the [100] repeat are offset such that the channel takes on a zigzag shape in order to accommodate zigzag ribbons of TMA molecules (two per cell), hydrogen bonded through the carboxyl groups in the 1- and 3-positions. The enclathrated TMA molecules are strictly ordered with respect to the TMA·H<sub>2</sub>O framework.

### Introduction

We report here the crystal structures of two hydrates of trimesic acid (TMA) that were uncovered during a survey of TMA compounds. The two structures are similar, both being based on a planar framework of hydrogen-bonded TMA and water molecules, with the planar arrays stacked so as to form channels containing guest molecules. In one structure, with empirical formula TMA· $\frac{5}{6}$ H<sub>2</sub>O, the channels are occupied by additional TMA molecules in an ordered array; in the other, TMA·H<sub>2</sub>O· $\frac{2}{3}$ PA (PA = picric acid), the PA molecules occupy the channels in a disordered fashion.

Both structures are somewhat unusual. TMA· $\frac{5}{6}$ H<sub>2</sub>O contains 12 molecules of TMA and 10 water molecules per unit cell, in space group  $P1$ ; in the picric acid complex, the chain of PA molecules has a different periodicity from the host framework, leading to additional, diffuse layer lines. Accordingly, we report the structure solutions and refinements in some detail.

\* Part I: Duchamp & Marsh (1969).

† Work done while on sabbatical leave at California Institute of Technology.

‡ Contribution No. 5428 from the Arthur Amos Noyes Laboratory of Chemical Physics. This investigation was supported in part by Public Health Service Research Grant No. GM 16966 from the National Institute of General Medical Sciences, National Institutes of Health.

### Experimental

Lozenges of TMA· $\frac{5}{6}$ H<sub>2</sub>O, with a characteristic dagger-like appearance, were obtained, together with  $\alpha$ -TMA [crystal structure reported by Duchamp & Marsh (1969)] and TMA·3H<sub>2</sub>O, on recrystallizing TMA from water. Optimum conditions for obtaining TMA· $\frac{5}{6}$ H<sub>2</sub>O were not determined.

TMA·H<sub>2</sub>O· $\frac{2}{3}$ PA was obtained by recrystallization of 25 ml of an aqueous solution containing a total of 4.3 mmol of TMA plus PA. When the TMA:PA ratio in these solutions was 3:1, the predominant product was orthorhombic crystals of TMA· $\frac{1}{4}$ PA, together with some straw-colored triclinic needles of TMA·H<sub>2</sub>O· $\frac{2}{3}$ PA; when the ratio was 1:2, the latter crystals predominated. The composition of these triclinic needles did not appear to vary with the composition of the parent solution, since identical diffraction photographs were obtained from different preparations.

Unit-cell dimensions for both crystals were measured from back-reflection Weissenberg photographs about all three axes, with Cu  $K\alpha$  radiation. The density of TMA· $\frac{5}{6}$ H<sub>2</sub>O was measured by suspension in toluene-C<sub>2</sub>H<sub>4</sub>Br<sub>2</sub> solution, and that of TMA·H<sub>2</sub>O· $\frac{2}{3}$ PA by suspension in a CCl<sub>4</sub>-toluene solution. Crystal data are collected in Table 1. Chemical analyses of both compounds were carried out by Galbraith Laboratories.

For  $\text{TMA} \cdot \frac{5}{6} \text{H}_2\text{O}$ , measured and calculated (in parentheses) values are: C 49.08 (48.00); H 3.58 (3.44); O, by difference, 47.34% (48.56%); for  $\text{TMA} \cdot \text{H}_2\text{O} \cdot \frac{2}{3} \text{PA}$ : C 44.50 (44.47); H 3.01 (3.13); O 49.38 (49.05); N 3.10% (3.35%).

Crystals of  $\text{TMA} \cdot \text{H}_2\text{O} \cdot \frac{2}{3} \text{PA}$  give a diffraction pattern consisting of two components: (1) the Bragg (sharp) reflections that characterize the unit cell described in Table 1 and (2) a series of diffuse reflections which we ascribe to the PA molecules being ar-

ranged without long-range order but with a considerable degree of short-range order (Fig. 1). The periodicity of the diffuse layer lines in the [001] direction is 16.5 (2) Å; the picric acid content of the complex inferred from the 2:9 ratio of the periodicities of the sharp and diffuse layer lines agrees well with that obtained

Table 1. Crystal data

$\text{TMA} \cdot \text{H}_2\text{O} \cdot \frac{2}{3} \text{PA}$	$\text{TMA} \cdot \frac{5}{6} \text{H}_2\text{O}$
$\text{C}_9\text{H}_8\text{O}_7 \cdot \frac{2}{3} (\text{C}_6\text{H}_3\text{N}_3\text{O}_7)$	$\text{C}_9\text{H}_6\text{O}_6 \cdot \frac{5}{6} \text{H}_2\text{O}$
FW 279.1	FW 225.1
Triclinic, $P\bar{1}$	Triclinic, $P1$
$Z = 2, F(000) = 287.6^*$	$Z = 12, F(000) = 1396$
$a = 18.269 (8) \text{ \AA}$	$a = 16.640 (1) \text{ \AA}$
$b = 8.852 (5)$	$b = 18.548 (1)$
$c = 3.642 (4)$	$c = 9.512 (1)$
$\alpha = 90.43 (8)^\circ$	$\alpha = 95.81 (1)^\circ$
$\beta = 92.59 (6)$	$\beta = 91.06 (4)$
$\gamma = 99.56 (5)$	$\gamma = 94.35 (1)$
$V = 580.1 (7) \text{ \AA}^3$	$V = 2911.3 (6) \text{ \AA}^3$
$D_x = 1.597 \text{ g cm}^{-3}$	$D_x = 1.545 \text{ g cm}^{-3}$
$D_m = 1.570$	$D_m = 1.553$
$\mu(\text{Mo K}\alpha) = 1.54 \text{ cm}^{-1}$	$\mu(\text{Mo K}\alpha) = 1.47 \text{ cm}^{-1}$

\* 236 without picric acid.

Table 2. Details of data collection and structure refinement

	$\text{TMA} \cdot \text{H}_2\text{O} \cdot \frac{2}{3} \text{PA}$	$\text{TMA} \cdot \frac{5}{6} \text{H}_2\text{O}$
Crystal size and shape	Needle	Prism, $0.06 \times 0.12 \times 0.24 \text{ mm}$
Direction of $\varphi$ axis	$2^\circ$ from $c^*$	$4^\circ$ from $a^*$
Diffractometer	Datex-automated	Syntex prototype, full-circle
Scan method	GE, quarter-circle	full-circle
	$\theta-2\theta, 1^\circ \text{ min}^{-1}$	$\theta-2\theta$ , speed adjusted to intensity
Background	30 s	$\frac{1}{2}$ scan time
Radiation	Mo $K\alpha$ (0.7107 Å)	graphite monochromator
$2\theta$ range	$4-60^\circ$	$2-46^\circ$
Number of reflections	3370	8019
Number of $F^2 > 0$	2840	6768
Standard reflections	500, $\bar{2}11, 122, 020, 101$	$08\bar{1}, 4\bar{2}0, 51\bar{1}$
Behavior		No significant variation
Quantity minimized		$\Sigma(F_o^2 - F_c^2)/\sigma(F_c^2)^2$
$\sigma^2(F^2)$		Counting statistics + $(0.02 \text{ scan})^2$

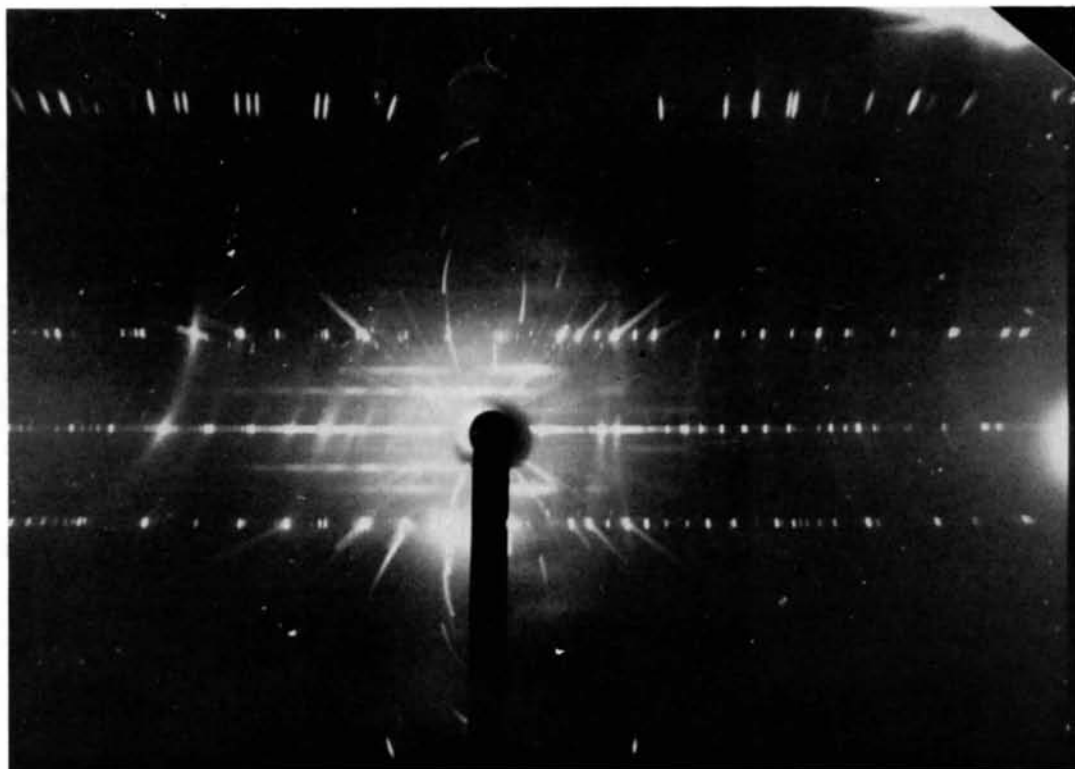


Fig. 1.  $\text{TMA} \cdot \text{H}_2\text{O} \cdot \frac{2}{3} \text{PA}$ . Oscillation photograph about [001] (Cu  $K\alpha$  radiation, Ni filter, 45 kV, 15 mA, 4 h), showing diffuse scattering associated with picric acid (PA) chains.

from the chemical analysis. However, the sharp and diffuse reciprocal lattices may not be exactly commensurate. Our structure determination is based entirely on the sharp reflections. While we made no test other than to check for anomalous background counts, we do not believe that the diffuse scattering (Fig. 1) interfered in any serious way with the intensity measurements of the sharp reflections.

Intensity data were measured at Caltech by standard techniques (see, e.g. Sherfinski & Marsh, 1973). Relevant information is summarized in Table 2. Neither compound showed a tendency toward twinning.

### Structure solution and refinement

#### TMA · H<sub>2</sub>O · $\frac{2}{3}$ PA

A three-dimensional Patterson map was interpreted in terms of space group  $P\bar{1}$ , with two TMA molecules hydrogen bonded together across a center of symmetry; a subsequent three-dimensional difference map indicated the location of the water molecule. However, least-squares refinement of this model was unsatis-

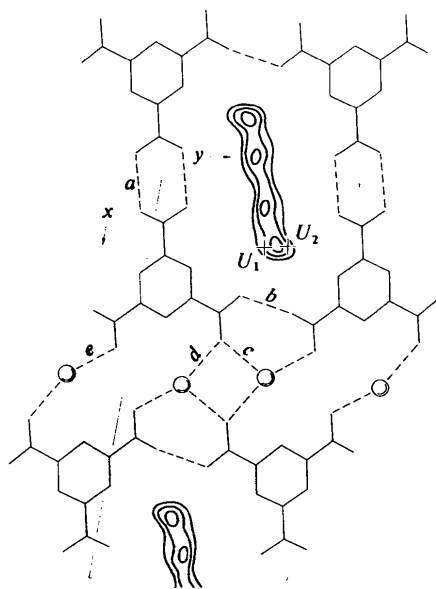


Fig. 2. Features of a difference projection for TMA · H<sub>2</sub>O ·  $\frac{2}{3}$ PA. The residual electron density, which represents the enclathrated picric acid molecules, is contoured at levels of 1.0, 2.0 and 3.0 e Å<sup>-2</sup>. Crosses (+) indicate the positions of the fractional atoms  $U_1$  and  $U_2$  which appear to be in register with the main framework; the remaining electron density was accounted for by the two-dimensional pseudo-atoms  $P$ ,  $Q$ ,  $R$ ,  $S$  and  $T$ . This diagram is also used to identify the hydrogen bonds ( $a$ – $e$ ) whose lengths are given in Table 8. In TMA · H<sub>2</sub>O ·  $\frac{2}{3}$ PA the molecules lie in the (111) planes and the hydrogen bonds do not lie in the plane of the projection but are directed as shown in Fig. 4. For TMA ·  $\frac{5}{6}$ H<sub>2</sub>O the present diagram serves as a slightly distorted representation of the arrangement in the layers of framework TMA and H<sub>2</sub>O molecules, as viewed along  $a$ .

factory. In particular, the  $hk0$  reflections showed continuing poor agreement; when the  $R$  index reached 0.133 for the 2840 reflections with  $F_o^2 > 0$ , the  $R$  index was 0.248 for the 460  $hk0$  reflections. A two-dimensional difference projection onto (001) (Fig. 2) indicated regions of residual electron density, and three-dimensional maps suggested that this electron density forms essentially continuous columns parallel to  $c$ . Presumably these columns represent the PA molecules occupying channels in the TMA · H<sub>2</sub>O framework.

In order to approximate the contribution of the PA molecules to the  $hk0$  reflections, additional 'atoms' were introduced. These 'atoms' were assigned the form factors of C and their coordinates  $x$  and  $y$ , and isotropic temperature factors  $B$  were adjusted on the basis of (001) difference maps; since they do not contribute to reflections with  $l \neq 0$ , no  $z$  coordinates were assigned.\* Eventually, five such 'atoms' –  $P$ ,  $Q$ ,  $R$ ,  $S$ , and  $T$  (Table 3) – were introduced.

At an intermediate stage of refinement, it became apparent that the H atom involved in the hydrogen bond between pairs of centrosymmetrically related TMA molecules is disordered between two sites; these two sites were assigned population factors of 0.7 and 0.3. There also appeared, on three-dimensional difference maps, small regions of residual electron density at the extremities of the columns identified as PA molecules and close to the TMA · H<sub>2</sub>O framework (Fig. 2). These regions presumably represent atoms that are at least partially in register with the TMA · H<sub>2</sub>O framework. They were treated as additional, fractional atoms with the form factors of O, and are identified as  $U_1$  and  $U_2$  in Table 4. We shall discuss their significance later.

Final refinement was by full-matrix least-squares adjustment of the parameters of the framework atoms, including  $U_1$  and  $U_2$ , based on all reflections with  $l \neq 0$ , interspersed with difference projections onto (001) from which the parameters of the two-dimensional 'atoms' were adjusted. In the least-squares calculations, a total of 176 parameters were adjusted: coordinates and

\* During some subsequent three-dimensional structure-factor calculations, each of these 'atoms' was divided into six equal parts with identical  $x$  and  $y$  coordinates and with  $z = 0, \frac{1}{6}, \frac{2}{6}, \frac{3}{6}, \frac{4}{6},$  and  $\frac{5}{6}$ . Since the maximum value of  $l$  is 5, this arrangement contributes only to reflections with  $l = 0$ .

Table 3. Parameters assigned to the two-dimensional pseudo-atoms

'Atom'	These 'atoms' were given the scattering factor of C.			
	$x$	$y$	Population factor	$B$ (Å <sup>2</sup> )
$P$	0.0155	0.513	0.45	5.0
$Q$	0.063	0.538	0.96	6.0
$R$	0.108	0.574	0.96	8.0
$S$	0.158	0.630	1.02	8.0
$T$	0.036	0.563	0.42	8.0



While these numbers are considerably larger than ideal, they are not surprising in view of the disorder and the obvious approximations that we have made in attempting to arrive at a reasonable model. Final positional parameters are listed in Tables 3 and 4.†

### TMA. $\frac{2}{3}$ H<sub>2</sub>O

The key to the solution of this structure lay in the extreme strength of reflections  $h00$  with  $h = 5n$ ; the  $E$  values are about 11.1 for 500, 7.9 for 10,0,0, and 4.8 for 15,0,0. Clearly, most of the atoms must lie in layers parallel to (100) and be separated by  $1/(5a^*)$ , or 3.32 Å. We further note that there is a close resemblance between the dimensions of the  $bc$  net ( $b = 18.55$ ,  $c =$

9.51 Å,  $\alpha = 95.8^\circ$ ) and the net formed by the [101] and [011] axes of TMA.H<sub>2</sub>O. $\frac{2}{3}$ PA ( $a' = 18.47$ ,  $b' = 9.55$  Å,  $\gamma' = 95.5^\circ$ ), which is the plane of the TMA.H<sub>2</sub>O framework in that compound. Finally, the  $u = 0$  section of a Patterson map showed a pattern of sharp peaks which quickly confirmed that the TMA.H<sub>2</sub>O arrays are similar in the two compounds and, moreover, that the five layers in TMA. $\frac{2}{3}$ H<sub>2</sub>O are virtually identical both in arrangement and orientation.

The complete solution of the TMA.H<sub>2</sub>O framework lay in deducing the in-plane displacements of these five planar motifs as they pack on top of one another; these displacements are manifested in large peaks on the Patterson sections  $u = 0.2$  and  $u = 0.4$ . Since each of the planar motifs is centrosymmetric (see Fig. 2), it seemed reasonable to presume that the stacking of motifs would maintain a center of symmetry and that the space group would be  $P\bar{1}$ ; it was only after considerable agonizing that we became convinced that no centrosymmetric structure could explain the arrangement of displacement vectors on the  $u = 0.2$  and  $u = 0.4$  sec-

† Lists of structure factors and thermal parameters for both compounds, and bond distances and angles for TMA. $\frac{2}{3}$ H<sub>2</sub>O have been deposited with the British Library Lending Division as Supplementary Publication No. SUP 32464 (60 pp.). Copies may be obtained through The Executive Secretary, International Union of Crystallography, 13 White Friars, Chester CH1 1NZ, England.

Table 6. *Coordinates (assumed) of the hydrogen atoms ( $\times 10^3$ )*

Asterisks indicate disordered hydrogen atoms that were assigned population factors of  $\frac{1}{2}$ . Isotropic temperature factors with  $B = 5.0 \text{ \AA}^2$  were assigned to hydrogen atoms bonded to C, and with  $B = 8.0 \text{ \AA}^2$  to those bonded to O.

	<i>x</i>	<i>y</i>	<i>z</i>	<i>x</i>	<i>y</i>	<i>z</i>	<i>x</i>	<i>y</i>	<i>z</i>	<i>x</i>	<i>y</i>	<i>z</i>
	<i>A</i>			<i>B</i>			<i>C</i>			<i>D</i>		
H(C2)	3	112	250	-3	-250	-336	200	32	161	204	-332	-435
H(C4)	6	313	117	-12	-456	-204	203	238	31	197	-534	-283
H(C6)	-2	134	-179	1	-280	93	198	59	-262	206	-349	-8
H(O1)*	-2	-36	-146	3	-106	58	203	-113	-234	202	-182	-37
H(O2)*	2	-49	82	1	-93	-169	204	-126	-6	202	-170	-265
H(O3)	19	218	527	-3	-361	-612	200	140	439	204	-441	-702
H(O5)	11	365	-194	0	-509	105	202	286	-276	204	-583	25
H(O7)	4	474	339	13	382	572	204	396	254	202	303	488
H(O7)	8	410	299	9	446	611	204	333	215	202	366	527
	<i>E</i>			<i>F</i>			<i>G</i>			<i>H</i>		
H(C2)	406	133	246	407	-228	-346	604	237	346	605	-125	-255
H(C4)	381	333	112	421	-435	-213	590	435	214	611	-329	-118
H(C6)	408	162	-174	405	-258	75	592	261	-81	603	-152	171
H(O1)*	403	-13	-148	400	-84	52	599	88	-55	603	17	147
H(O2)*	400	-27	78	403	-72	-173	604	74	175	598	32	-81
H(O3)	395	238	521	427	-335	-626	576	340	619	614	-234	-527
H(O5)	384	387	-202	407	-483	91	597	490	-99	618	-384	187
H(O7)	413	498	326	382	405	562	615	600	422	592	506	662
H(O7)	407	434	288	388	470	600	608	535	384	600	571	699
	<i>I</i>			<i>J</i>			<i>K</i>			<i>L</i>		
H(C2)	801	336	429	807	-34	-161	344	-185	334	632	175	657
H(C4)	789	527	286	807	-238	-27	95	-183	329	882	180	652
H(C6)	806	350	1	802	-59	266	236	-3	495	735	-1	506
H(O1)*	798	180	37	801	116	236	433	32	529	547	-39	476
H(O2)*	802	173	268	796	125	13	489	-63	442	493	56	558
H(O3)	798	441	698	803	-140	-437						
H(O4)							159	-335	267	827	328	716
H(O5)	792	578	-30	806	-286	281						
H(O5)*							-19	-63	432	1000	55	566
H(O6)*							52	30	538	927	-38	456
H(O7)	804	694	512	784	600	737						
H(O7)	799	632	470	789	662	779						

tions. Interpretation of the displacement vectors in space group  $P1$  led to approximate positions for 150 C and O atoms comprising 10 TMA units. The resulting  $R$  index was 0.53 for 1500 reflections with  $\sin^2 \theta/\lambda^2 \leq 0.1$ , and dropped to 0.35 for 3708 reflections when the 10 framework  $\text{H}_2\text{O}$  molecules and the two additional 'guest' TMA molecules were added on the basis of electron density maps. Preliminary refinement was by structure-factor difference-map calculations, from which the coordinates and many of the pronounced temperature-factor anisotropies were adjusted. After five such cycles, the  $R$  index was 0.18 for 5600 reflections out to  $\sin^2 \theta/\lambda^2 = 0.25$ .

Block-diagonal least-squares refinement was then initiated, first for the coordinates and later for the anisotropic temperature factors. H atoms were included in the structure factors at assumed positions, but were not refined. Since the C(7)—O(1) and C(7)—O(2) bond lengths were consistently more nearly equal than those in the other two carboxyl groups, we presumed that, as in  $\text{TMA} \cdot \text{H}_2\text{O} \cdot \frac{2}{3}\text{PA}$ , the H atom is disordered between two sites; in this case, for computational convenience, we assigned population factors of 0.5 to each site.

Convergence was very slow because of the large number of matrices (eventually, 190  $3 \times 3$  matrices for the coordinates and 190  $6 \times 6$  matrices for the thermal parameters) and the large correlations, particularly among the thermal parameters, caused by the hypersymmetry of the structure. Various shift factors and extrapolation functions were applied in attempts to hasten the process; as usual, however, such devices seemed more valuable in hindsight than in foresight. Each least-squares cycle required approximately 32 min on an IBM 370/158 computer, and 11 cycles were carried out. Complete convergence was not reached; during the last cycle, 18 parameters shifted by more than  $1.0\sigma$ , and one of them, the  $x$  coordinate of a water O atom, by slightly more than  $2.0\sigma$ . The average shift-to-sigma ratio was 0.3, the  $R$  index was 0.112 for 6768 reflections with positive net intensity, and the goodness-of-fit was 1.33 for  $n = 8019$  reflections in the data set, including those with negative net intensity, and  $p = 1710$  parameters adjusted. The atomic parameters are in Tables 5 and 6.\*

## Results and discussion

### Molecular dimensions

Selected dimensions of the TMA molecule in the two structures are given in Fig. 3. For  $\text{TMA} \cdot \text{H}_2\text{O} \cdot \frac{2}{3}\text{PA}$  the formal e.s.d.'s are approximately  $0.003 \text{ \AA}$  in the bond lengths and  $0.2^\circ$  in the angles; however, the agreement among chemically equivalent values suggests that these

values might be doubled. For  $\text{TMA} \cdot \frac{5}{6}\text{H}_2\text{O}$  the values are averaged over the ten molecules  $A-J$  of the main framework; agreement among equivalent values suggests e.s.d.'s of about  $0.02 \text{ \AA}$  and  $1.1^\circ$  for a single measurement, about 75% larger than predicted from the formal e.s.d.'s (which neglect the severe blocking of the least-squares matrices and the incomplete convergence). On the assumption that all ten molecules are equivalent, the e.s.d.'s in the average values given in Fig. 3 are about  $0.006 \text{ \AA}$  and  $0.4^\circ$ .

The C—C distances are closely equal in all three forms of TMA that have been studied (Table 7). The average C—C(external) distance,  $1.487(1) \text{ \AA}$ , is slightly smaller than the value  $1.491(1) \text{ \AA}$  obtained by Domenicano, Vacigo & Coulson (1975, Table 3)

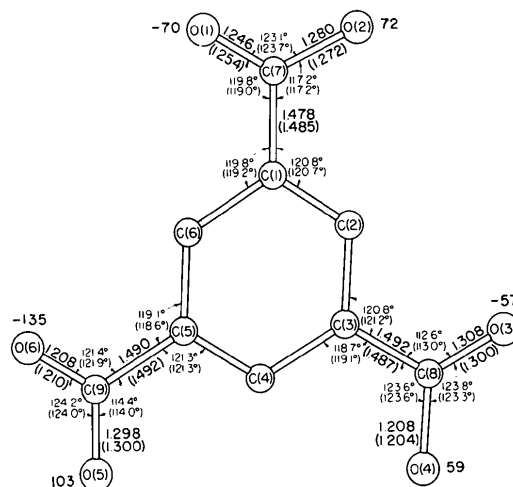


Fig. 3. Some bond distances ( $\text{\AA}$ ) and angles ( $^\circ$ ). Upper values refer to  $\text{TMA} \cdot \text{H}_2\text{O} \cdot \frac{2}{3}\text{PA}$  and carry e.s.d.'s of approximately  $0.006 \text{ \AA}$  and  $0.4^\circ$  (see text); values in parentheses are averages of the 10 framework molecules in  $\text{TMA} \cdot \frac{5}{6}\text{H}_2\text{O}$ . The figures adjacent to the O atoms give the deviations (units of  $10^{-3} \text{ \AA}$ ) of these atoms from the best plane of the C atoms in  $\text{TMA} \cdot \text{H}_2\text{O} \cdot \frac{2}{3}\text{PA}$ . The dihedral angles between the plane of the C atoms and the planes of the several carboxyl groups are as follows: at C(1)  $-3.7^\circ$ ; at C(3)  $-3.0^\circ$ ; at C(5)  $+6.2^\circ$ . The deviations from planarity and the dihedral angles in the TMA molecules in  $\text{TMA} \cdot \frac{5}{6}\text{H}_2\text{O}$  are not given in detail but are similar to the values found for  $\text{TMA} \cdot \text{H}_2\text{O} \cdot \frac{2}{3}\text{PA}$ .

Table 7. Mean C—C distances in various TMA compounds

Values in parentheses are standard deviations of the mean values, evaluated from the spread among the  $n$  individual values.

	$\text{TMA} \cdot \text{H}_2\text{O} \cdot \frac{2}{3}\text{PA}$	$\text{TMA} \cdot \frac{5}{6}\text{H}_2\text{O}$	$\alpha\text{-TMA}^*$
C—C (ring)	1.390 (2) $\text{\AA}$	1.388 (2) $\text{\AA}$	1.390 (1) $\text{\AA}$
C—C (external)	1.487 (3)	1.486 (3)	1.488 (2)
$n$	6,3	72,36	36,18

\* See deposition footnote.

\* Duchamp & Marsh (1969)

as a mean value for the exocyclic C—C bond length in a variety of substituted benzene derivatives. In hemimellitic acid dihydrate (Mo & Adman, 1975) the exocyclic C—C bond lengths are 1.489 (2) and 1.493 (2) Å for the two carboxyl groups approximately in the benzene ring plane.

In  $\text{TMA} \cdot \text{H}_2\text{O} \cdot \frac{2}{3}\text{PA}$  the nine C atoms of the TMA molecule are coplanar within experimental error; the carboxyl groups are rotated by small angles with respect to the plane of the C atoms (Fig. 3). In  $\text{TMA} \cdot \frac{5}{6}\text{H}_2\text{O}$ , the benzene rings of the twelve independent TMA molecules are all planar but many of the carboxyl groups are slightly tilted out of the ring planes as well as twisted. However, the resultant deviations from planarity are all small, the largest being that of O(6)G,  $-0.324$  Å. There is no difference between the pattern of tilts and twists found for the framework molecules *A–J* and for the enclathrated molecules *K, L*.

In both compounds the carboxyl groups involving C(8) and C(9) are hydrogen bonded to water molecules and are ordered; there are pronounced differences in the bond lengths [C=O, 1.207 (3); C—O(H), 1.301 (3) Å] and angles [C—C=O, 123.1 (3); C—C—O(H), 113.5 (3)°] within these carboxyl groups. In addition, the exocyclic C—C—C bond angles are unequal, the smaller angles C(4)—C(3)—C(8) and C(6)—C(5)—C(9) being *cis* to the C=O grouping. On the other hand, the carboxyl groups at C(7), which are dimerized across centers of symmetry in  $\text{TMA} \cdot \text{H}_2\text{O} \cdot \frac{2}{3}\text{PA}$  and across pseudocenters in  $\text{TMA} \cdot \frac{5}{6}\text{H}_2\text{O}$ , are partly disordered and the C(7)—O(1) and C(7)—O(2) distances are more nearly equal at 1.250 (4) and 1.276 (4) Å. Difference maps of  $\text{TMA} \cdot \text{H}_2\text{O} \cdot \frac{2}{3}\text{PA}$  indicate two partially occupied sites for the H atom, and we assigned population factors of 0.7 for the site closest to O(2) and 0.3 to the site closest to O(1). We note that the

hydrogen-bond angle C(7)—O(1)⋯O(2') of 121.8° is less favorable than the C(7)—O(2)⋯O(1') angle of 115.2°, which probably accounts for the different population factors. Similar features appear in  $\text{TMA} \cdot \frac{5}{6}\text{H}_2\text{O}$  but are less firmly established because of the incomplete refinement.

The pattern of temperature-factor anisotropy is remarkably consistent among all the TMA molecules in both compounds, in that the largest mean-square displacements *U* are in directions perpendicular to the plane of the particular molecule, and the out-of-plane displacements of the O atoms are two or three times larger than those of the C atoms. This trend holds as well for the water molecules in the  $\text{TMA} \cdot \text{H}_2\text{O}$  sheets. Similar features appear in the temperature parameters of  $\alpha$ -TMA (Duchamp & Marsh, 1969), hemimellitic acid dihydrate (Mo & Adman, 1975) and isophthalic acid (Alcala & Martinez-Carrera, 1972). The enhanced displacement amplitudes of the carboxyl O atoms could well be due to libration of the carboxyl groups about the C(ring)—C(carboxyl) bonds, as was invoked to explain the large vibration amplitudes of O atoms in nitro groups (Trueblood, Goldish & Donohue, 1961; Dunitz & White, 1973); the displacement amplitudes of the water molecules could represent simple out-of-plane vibrations, since all of the restraining hydrogen bonds lie in-plane.

Both structures are based on the same overall molecular arrangement — parallel layers of composition  $\text{TMA} \cdot \text{H}_2\text{O}$  with all available protons involved in O—H⋯O hydrogen bonds. The hydrogen-bond lengths are given in Table 8; these distances are significantly shorter, by about 0.25 Å, where the carboxyl group is the donor than those where the water molecule is the donor. The hydrogen-bond lengths in  $\text{TMA} \cdot \frac{5}{6}\text{H}_2\text{O}$  vary considerably, but the average values

Table 8. *Hydrogen-bond distances (O⋯O; Å) in the two structures*

The bonds are labeled in Fig. 2; see also Fig. 4. Numbers in parentheses are e.s.d.'s obtained from the structure determination; numbers in square brackets are r.m.s. deviations from the means.

	<i>a</i>	<i>b</i>	<i>c</i>	<i>d</i>	<i>e</i>
$\text{TMA} \cdot \text{H}_2\text{O} \cdot \frac{2}{3}\text{PA}$	2.653 (5)	2.646 (5)	2.888 (5)	2.892 (5)	2.604 (5)
$\text{TMA} \cdot \frac{5}{6}\text{H}_2\text{O}$					
<i>A</i>	2.63	2.62	2.84	2.80	2.59
<i>B</i>	2.66	2.68	2.94	2.87	2.57
<i>C</i>	2.65	2.63	2.86	2.84	2.58
<i>D</i>	2.63	2.56	2.86	2.81	2.56
<i>E</i>	2.66	2.62	2.89	2.90	2.65
<i>F</i>	2.65	2.67	2.91	2.89	2.59
<i>G</i>	2.63	2.69	2.85	2.91	2.62
<i>H</i>	2.63	2.66	2.91	2.88	2.59
<i>I</i>	2.62	2.53	2.78	2.75	2.61
<i>J</i>	2.66	2.65	2.90	2.85	2.56
Average	2.641 [15]	2.632 [52]	2.874 [44]	2.850 [52]	2.592 [29]
<i>K</i>	2.65	2.64*			
<i>L</i>	2.65	2.60*			

\* O(5)⋯O(6)

do not differ appreciably from those found in  $\text{TMA} \cdot \text{H}_2\text{O} \cdot \frac{2}{3}\text{PA}$ . As can be seen in Fig. 2, this hydrogen-bond arrangement results in a cavity within each  $\text{TMA} \cdot \text{H}_2\text{O}$  layer; when these layers are stacked on top of one another a channel develops in which is enclathrated a picric acid molecule in  $\text{TMA} \cdot \text{H}_2\text{O} \cdot \frac{2}{3}\text{PA}$  and an additional TMA molecule in  $\text{TMA} \cdot \frac{5}{6}\text{H}_2\text{O}$ . Details of the stacking and the enclathration are different in the two compounds, and are discussed separately.

#### $\text{TMA} \cdot \text{H}_2\text{O} \cdot \frac{2}{3}\text{PA}$

The hydrogen-bonded  $\text{TMA} \cdot \text{H}_2\text{O}$  sheets (Fig. 4) are parallel to the  $(\bar{1}\bar{1}1)$  planes. Each individual TMA molecule makes an angle of  $5.0^\circ$  with these planes, so that the sheets are slightly puckered. The normal to the  $(\bar{1}\bar{1}1)$  planes makes an angle of  $24.8^\circ$  with  $c$ , and adjacent sheets are separated by  $3.31 \text{ \AA}$ ; molecules separated by translation along  $c$  are stacked in a graphite-like manner (Fig. 5).

The chains of enclathrated PA molecules are oriented parallel to  $c$ , with a periodicity (derived from the spacing of the diffuse layer lines) of  $16.5 \text{ \AA}$ . The chemical composition (see *Experimental*) requires that there be two PA molecules, with different orientations, within the repeat distance of  $16.5 \text{ \AA}$ ; consideration of molecular models indicates that two molecules could

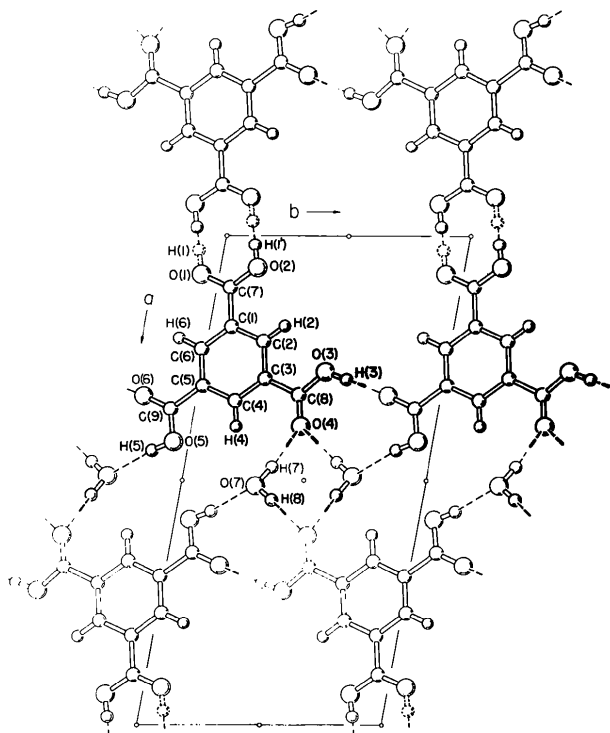


Fig. 4. The framework structure of  $\text{TMA} \cdot \text{H}_2\text{O} \cdot \frac{2}{3}\text{PA}$ , as viewed along  $c^*$ . As the TMA and  $\text{H}_2\text{O}$  molecules lie approximately in the  $(\bar{1}\bar{1}1)$  planes, the hydrogen bonds are directed out of the  $(001)$  plane shown in the figure.

comfortably occupy this length of channel. According to this interpretation, there are two repeating units along the PA chain, or four PA molecules, for every nine  $\text{TMA} \cdot \text{H}_2\text{O}$  layers.\* At first glance it seems somewhat surprising that the PA chain has a repeat distance of two molecules; that is, that alternate molecules within the chain have similar orientations. However, the appearance of the sites  $U$ , with population factors close to  $\frac{2}{3}$ , suggest that the PA molecules maintain partial registry with the main  $\text{TMA} \cdot \text{H}_2\text{O}$  framework, and such registry would dictate a repeating structure along the chain. Site  $U_1$  lies about  $2.9 \text{ \AA}$  from the hydroxyl atom  $\text{O}(3)$  while site  $U_2$  lies  $3.0 \text{ \AA}$  from both  $\text{O}(3)$  and  $\text{C}(5)$ , distances that indicate appreciable interaction. It seems unlikely that these  $U$  sites represent additional water molecules, since in that case the calculated densities and chemical compositions would be in worse agreement with the experimental values; we think it more likely that they are O atoms of the PA molecules, held in loose association with the main framework. Further studies of the diffuse reflections would be necessary for a more complete understanding of the details of the PA chain.

#### $\text{TMA} \cdot \frac{5}{6}\text{H}_2\text{O}$

The  $\text{TMA} \cdot \text{H}_2\text{O}$  layers are parallel to the  $(100)$  planes, and are separated by an average of  $3.32 \text{ \AA}$  — essentially the same as the separation of  $3.31 \text{ \AA}$  in the PA compound. Individual TMA molecules are inclined

\* An electron count based on the population factors of sites  $P$ ,  $Q$ ,  $R$ ,  $S$ ,  $T$  and  $U$  leads to approximately  $0.46$  molecules of picric acid per unit cell, satisfactorily close to  $\frac{2}{3}$ .

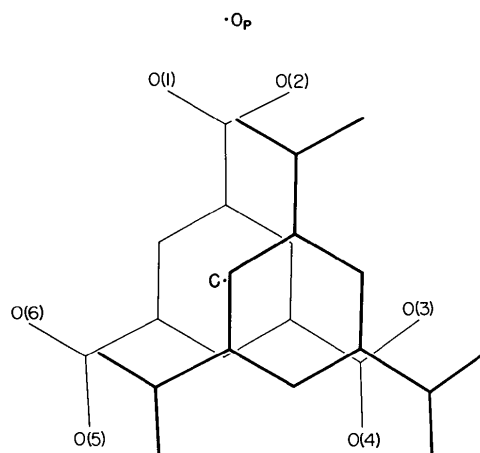


Fig. 5.  $\text{TMA} \cdot \text{H}_2\text{O} \cdot \frac{2}{3}\text{PA}$ . Overlap diagram of two TMA molecules separated by translation along  $c$ ; the molecules are viewed normal to the plane of the C atoms, the translated molecule being closer to the observer. The centroid of the reference molecule, the coordinates of which are given in Table 4, is denoted by  $C$  and the origin of the unit cell, projected onto the molecular plane, is shown by  $Op$ . The O atoms of the reference molecule are labeled for convenience.



to the (100) plane by angles ranging from  $1.9^\circ$  for molecule *C* to  $5.8^\circ$  for molecule *E*. The arrangement of atoms in each of the five layers is closely similar to that in  $\text{TMA} \cdot \text{H}_2\text{O} \cdot \frac{2}{3}\text{PA}$  (Fig. 4), with minor differences in such details as twists and tilts of the exocyclic C—C bonds and out-of-plane displacements of the water molecules. These differences presumably are accommodations involving the enclathrated TMA molecules.

The enclathrated molecules *K* and *L* are hydrogen bonded together, in the manner typical of carboxylic acid groups, so as to form chains parallel to **a** (Fig. 6); the four O...O distances are statistically equal (see Table 8). We have assumed, by analogy with the  $\text{TMA} \cdot \text{H}_2\text{O}$  layers, that these hydrogen bonds are disordered, and have assigned population factors of 0.5 to the H atoms bonded to O(1), O(2), O(5) and O(6). The zigzag ribbons of hydrogen-bonded *K* and *L* molecules are very similar to the ribbons of hydrogen-bonded molecules found in crystalline isophthalic acid (1,3-benzenedicarboxylic acid) (Alcala & Martinez-Carrera, 1972); in isophthalic acid the hydrogen bonds are ordered.

The specifics of the interactions between the enclathrated chains and the host network of  $\text{TMA} \cdot \text{H}_2\text{O}$  layers are not clear. They probably include weak hydrogen bonds or electrostatic forces involving the remaining carboxyl atoms O(3) and O(4) on molecules *K* and *L*. Each of these atoms is neighbored by at least two O atoms, at distances of 2.9–3.1 Å, of the main network; the geometries of these interactions do not suggest directed hydrogen bonding. We are not sure which of the carboxyl O atoms is protonated. The C(8)—O(4) distances in the two molecules are slightly longer (average, 1.31 Å) than the C(8)—O(3) distances

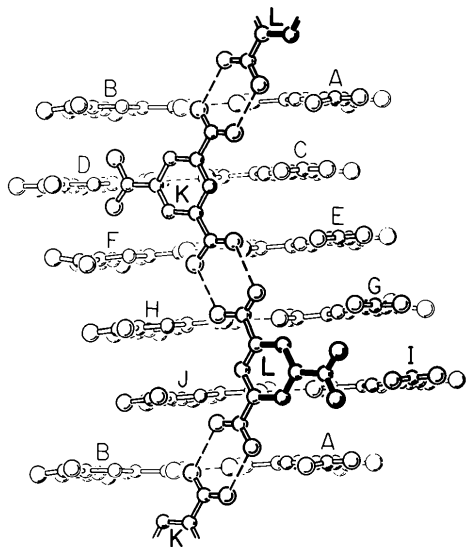


Fig. 6. The structure of  $\text{TMA} \cdot \frac{2}{3}\text{H}_2\text{O}$ , showing the chains of enclathrated molecules *K* and *L* and the zigzag stacking of framework molecules *A*–*J*. The view is along  $c^*$ , with **a** vertical.

(1.25 Å), and on this basis we assigned the protons to O(4), but perhaps there is disorder here as well.

A surprising characteristic of the structure of  $\text{TMA} \cdot \frac{2}{3}\text{H}_2\text{O}$  is its inability to achieve any symmetry (other than translational) despite the incorporation of 12 molecules in the unit cell. The situation seems even more remarkable when one considers that each of the five  $\text{TMA} \cdot \text{H}_2\text{O}$  layers is closely centrosymmetric, as is the chain of enclathrated molecules *K* and *L*. Moreover, the approximate centers of symmetry between molecules *K* and *L* closely coincide with the approximate centers that involve molecules *C*, *D*, *E*, *F*, *G*, *H*, *I* and *J* (Fig. 6). In other words, the structure differs from the symmetry of  $P\bar{1}$  only in the relationship of the  $\text{TMA} \cdot \text{H}_2\text{O}$  layer involving molecules *A* and *B* with the rest of the structure; this layer is displaced by approximately 0.5 Å from the centrosymmetric position.

As we understand them, the exigencies leading to this pseudocentrosymmetric arrangement are as follows. The strong, hydrogen-bond interactions between the 1- and 3-carboxyl groups in molecules *K* and *L* result in a zigzag chain that has a repeat distance five times as long as the spacing between successive  $\text{TMA} \cdot \text{H}_2\text{O}$  layers. In order to accommodate this intercalated chain, the successive  $\text{TMA} \cdot \text{H}_2\text{O}$  layers must also form a zigzag array which, in repeating after five layers, must comprise three 'zigs' and two 'zags'; thus, each zag must involve, on the average, a displacement of adjacent layers by 50% more than the displacement in an average zig. Each of the three zigs involves a displacement of about 1.6 Å and results in a stacking of TMA molecules analogous to that found in graphite, with the center of the benzene ring approximately above a ring C atom in the preceding layer; in such an arrangement, there is no superposition of covalent bonds. However, the increased displacement that would be associated with two equal zags of 2.4 Å would result in an unfavorable overlap with approximate superposition of five pairs of bonds; accordingly, one of the zags (between layers *AB* and *CD*) is relatively small at 1.9 Å, leading again to graphite-like superposition, while the other zag (layers *IJ* and *AB*) is large, 2.9 Å, and also avoids serious bond–bond overlaps. The unequal component of these two zags precludes a center of symmetry.

The essential structural unit in both these crystals is the planar hydrogen-bonded layer of composition  $\text{TMA} \cdot \text{H}_2\text{O}$ ; the essential feature of the arrangement of TMA and  $\text{H}_2\text{O}$  molecules in such a layer is the gap left between the molecules, large enough to allow insertion of a chain of enclathrated molecules of the approximate size and shape of TMA. The bonding between such layers is appreciably weaker than within the layers, and consequently the layers can be shifted laterally in order to accommodate guests of different types. Accommodation of the zigzag ribbon of enclathrated TMA molecules requires appropriate shifts of adjacent  $\text{TMA} \cdot \text{H}_2\text{O}$  layers. The picric acid molecule, on the

other hand, does not have regions capable of strong intermolecular bonding [there is presumably intramolecular hydrogen bonding as in anthracene-picric acid (Herbstein & Kaftory, 1975)] and thus fits without difficulty into a linear channel.

A somewhat similar structural situation has recently been reported for the ion-radical salt (TMTTF)<sub>1.3</sub>(TCNQ)<sub>2</sub> (Kistenmacher, Phillips, Cowan, Ferraris, Bloch & Poehler, 1976) (TMTTF is 4,4',5,5'-tetramethyl-2,2'-bis-1,3-dithiole and TCNQ is 7,7,8,8-tetracyano-*p*-quinodimethane). However, many features of the diffraction patterns from (TMTTF)<sub>1.3</sub>(TCNQ)<sub>2</sub> differ from those we have encountered.

The overall structural resemblance among these three compounds suggests that they can be formulated in a similar way—TMA·H<sub>2</sub>O·[ $\frac{2}{3}$ PA], TMA·H<sub>2</sub>O·[ $\frac{1}{5}$ TMA] and (TMTTF)<sub>1.3</sub>(TCNQ)<sub>2</sub>·[0.3TMTTF], where the square brackets indicate the enclathrated molecules and the rest of the formula the framework structure.

All computations were carried out on the IBM 370/158 computer at Caltech with the CRYM system of programs (Duchamp, Trus & Westphal, 1969). We thank Dr Sten Samson for help with the measurements

and Mrs Jean Westphal for help with programming. FHH is indebted to REM for his hospitality during sabbatical leave at Caltech.

#### References

- ALCALA, R. & MARTÍNEZ-CARRERA, S. (1972). *Acta Cryst.* B28, 1671–1677.  
 DOMENICANO, A., VACIAGO, A. & COULSON, C. A. (1975). *Acta Cryst.* B31, 221–234.  
 DUCHAMP, D. J. & MARSH, R. E. (1969). *Acta Cryst.* B25, 5–19.  
 DUCHAMP, D. J., TRUS, B. L. & WESTPHAL, J. (1969). Unpublished results.  
 DUNITZ, J. D. & WHITE, J. D. N. (1973). *Acta Cryst.* A29, 93–94.  
 HERBSTEIN, F. H. & KAFTORY, M. (1975). *Acta Cryst.* B32, 387–396.  
 KISTENMACHER, T. J., PHILLIPS, T. E., COWAN, D. O., FERRARIS, J. P., BLOCH, A. N. & POEHLER, T. O. (1976). *Acta Cryst.* B32, 539–547.  
 MO, F. & ADMAN, E. (1975). *Acta Cryst.* B31, 192–198.  
 SHERFINSKI, J. S. & MARSH, R. E. (1973). *Acta Cryst.* B29, 192–198.  
 TRUEBLOOD, K. N., GOLDISH, E. & DONOHUE, J. (1961). *Acta Cryst.* 14, 1009–1017.

*Acta Cryst.* (1977). B33, 2367–2372

## Structure and Charge Distribution of Oxamide as Determined from High-Order X-ray Data\*

BY G. DE WITH AND S. HARKEMA

*Chemical Physics Laboratory, Twente University of Technology, PO Box 217, Enschede, The Netherlands*

(Received 3 December 1976; accepted 24 January 1977)

The crystal structure and electronic charge distribution of oxamide (oxalic acid diamide, C<sub>2</sub>N<sub>2</sub>O<sub>2</sub>H<sub>4</sub>) have been determined at 293 K by X-ray methods. The structural results of Ayerst & Duke [*Acta Cryst.* (1954), 7, 588–590] have been confirmed. High-order data [up to  $(\sin \theta)/\lambda = 1.15 \text{ \AA}^{-1}$ ] were collected. A clear indication of bonding features is obtained. The effect of data cut-off on the difference density map has been investigated.

### Introduction

Although three earlier X-ray determinations have been performed for the triclinic form of oxamide (Misch & van der Wijk, 1938; Romers, 1953; Ayerst & Duke, 1954), none is accurate enough to show an indication of bonding features in the resulting difference-Fourier

map. At present, however, it is possible to obtain X-ray results which do show reliable bonding features (see, e.g., Stevens & Hope, 1975). A determination of the charge distribution was therefore carried out by means of X-ray methods.

### Experimental

Oxamide crystals were grown from formamide by slow evaporation of a saturated solution kept at 363 K. Frequently the crystals showed twinning [as was expected

\* Part of this research has been carried out under the auspices of the Foundation for Fundamental Research on Matter by Electrons and X-rays (FOMRE), and with aid from the Netherlands Organization for Advancement of Pure Research (ZWO).